Neuron, Volume *95*

Supplemental Information

Stable Positioning of Unc13 Restricts Synaptic Vesicle Fusion to Defined Release Sites to Promote Synchronous Neurotransmission

Suneel Reddy-Alla, Mathias A. Böhme, Eric Reynolds, Christina Beis, Andreas T. Grasskamp, Malou M. Mampell, Marta Maglione, Meida Jusyte, Ulises Rey, Husam Babikir, Anthony W. McCarthy, Christine Quentin, Tanja Matkovic, Dominique Dufour Bergeron, Zeeshan Mushtaq, Fabian Göttfert, David Owald, Thorsten Mielke, Stefan W. Hell, Stephan J. Sigrist, and Alexander M. Walter

Inventory of supplemental information

Movie 1: live movie of GCaMP fluorescence – related to Figure 1

Movie 1 shows a 34 s excerpt from a stabilized GCaMP recording in real time in which action potentials were evoked. Data like these were used for Figures 1I-L; 2 and S2.

Figure S1 – related to Figure 1

Figure S1 provides long-term FRAP analysis of motoneuronally overexpressed Unc13A-GFP and thus complements the short-term FRAP data of Figure 1M-Q.

Figure S2 – related to Figure 2

Figure S2 shows GCaMP-based single active zone measurements of spontaneous and evoked activity in correlation to levels of BRP and Unc13A and complements the data shown in Fig 2.

Figure S3 – related to Figure 3

Figure S3 provides confocal and STED analysis of motoneuronally overexpressed N-term-GFP as well as C-term-GFP and thus complements the analysis provided in Figure 3C-F.

Figure S4 – related to Figure 4

Figure S4 shows that the overexpression of the N-term-GFP fragment displaces endogenous Unc13 from the AZ. These data help to interpret the reduced number of release sites shown in Figure 4K,L.

Figure S5 – related to Figure 5

Figure S5 shows the effect of mutating the CaM-binding site of Unc13A on synaptic transmission. This mutation does not phenocopy the effects observed upon rescue with the C-term-GFP fragment, suggesting that loss of the CaM domain in the C-term-GFP is not causative for the effects observed in Figure 5.

Figure S6 – related to Figure 5

Figure S6 shows that expression of the C-term-GFP fragment in the *unc13*^{null} background redistributes RBP, but neither Syx-1A nor Unc18 from the AZ and characterizes an additional phenotype of this genotype.

Figure S7 – related to Figure 6

Figure S7 shows the full 60 Hz trains of C-term-GFP rescue with and without EGTA as in Fig. 6 only the responses to the first 20 APs are shown. Furthermore, Figure S7 also shows that the large facilitation observed in the C-term-GFP rescue (Figure 6C) was mainly caused by an increase in the asynchronous release component which could be inhibited by EGTA incubation.

Figure S8 – related to Figure 6

Figure S8 shows that a higher stimulation frequency of 100 Hz compared to the 60 Hz train investigated in Figures 6 and S7 further increased the contribution of asynchronous release and the delay in transmission. Furthermore, analysis with linear fits to cumulative responses reveals that *unc13*^{null} larvae expressing the C-term-GFP fragment have comparable back-extrapolated y-intercepts but slowed forward priming.

Table S1 – related to all figures including supplemental figures

Table S1 provides all Figure source data, number of experiments, P values and the nature of the statistical comparisons used in this study.

Supplementary figures and legends

Figure S1 – related to Figure 1

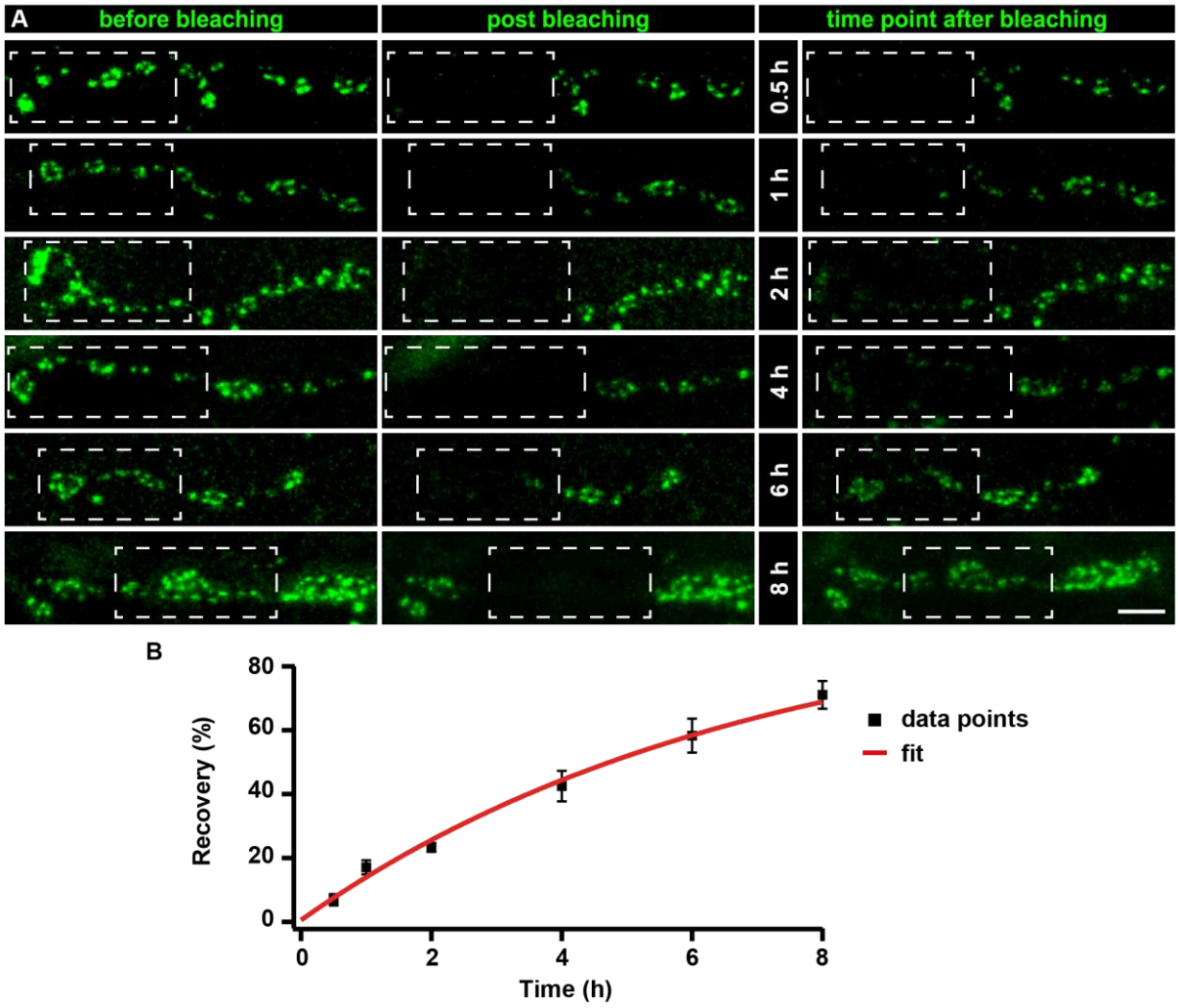

Figure S1: Unc13A recovers within hours

(A) Long-term FRAP of motoneuronally overexpressed Unc13A-GFP of muscle 26/27. Dashed box shows bleached bouton before and directly after the fluorescence bleaching. Fluorescence recovery was measured 0.5; 1; 2; 4; 6 or 8 h after bleaching. Different time points were measured in different animals. **(B)** Quantification of recovery (%) over time. Bleached Unc13A-GFP showed a slow fluorescence recovery, exhibiting a tau of 6.88 ± 0.55 h, single exponential recovery fit. Figure source data are listed in **Supplementary Table 1**. Data are mean ± s.e.m. Scale bar 5 µm.

Figure S2 – related to Figure 2

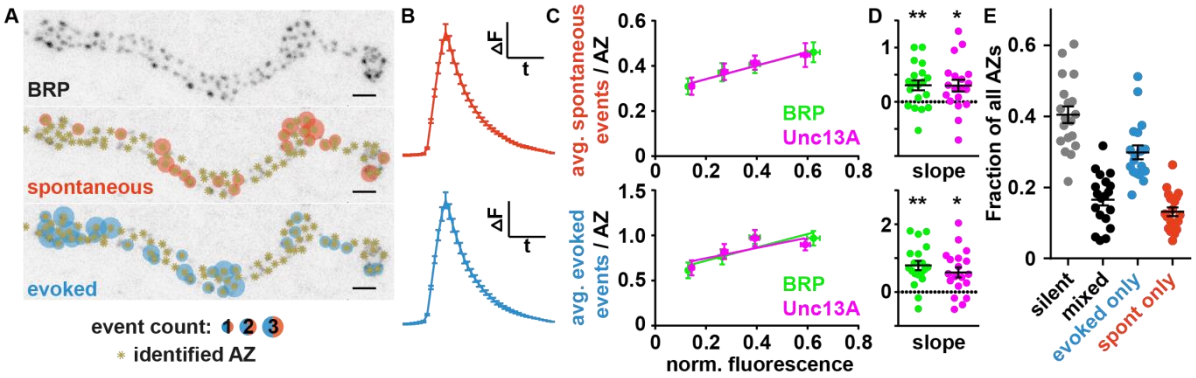

Figure S2: GCaMP-based single active zone measurements of spontaneous and evoked activity

(A) Inverted confocal image of BRP staining overlaid with asterisks to mark identified AZ positions and with circles corresponding to number of spontaneous/evoked events, measured in GCaMP experiments. **(B)** Average GCaMP fluorescence changes induced by spontaneous (top) and evoked (bottom) events at all imaged NMJs. (Average of all animals). **(C)** Top: average number of spontaneous events per AZ plotted against normalized, local fluorescence levels of BRP and Unc13A. Bottom: same for evoked events. **(D)** Slopes of linear fits on measurements in individual NMJs. Stars indicate statistically significant deviation from zero. **(E)** Quantification of release modes shown in all NMJs. Silent: no activity; mixed: both spontaneous and evoked activity; evoked/spont only: only one release mode observed. All panels show mean ± s.e.m. Figure source data, number of experiments and P values are listed in **Supplementary Table 1**. Scale bars: 2 µm.

Figure S3 – related to Figure 3

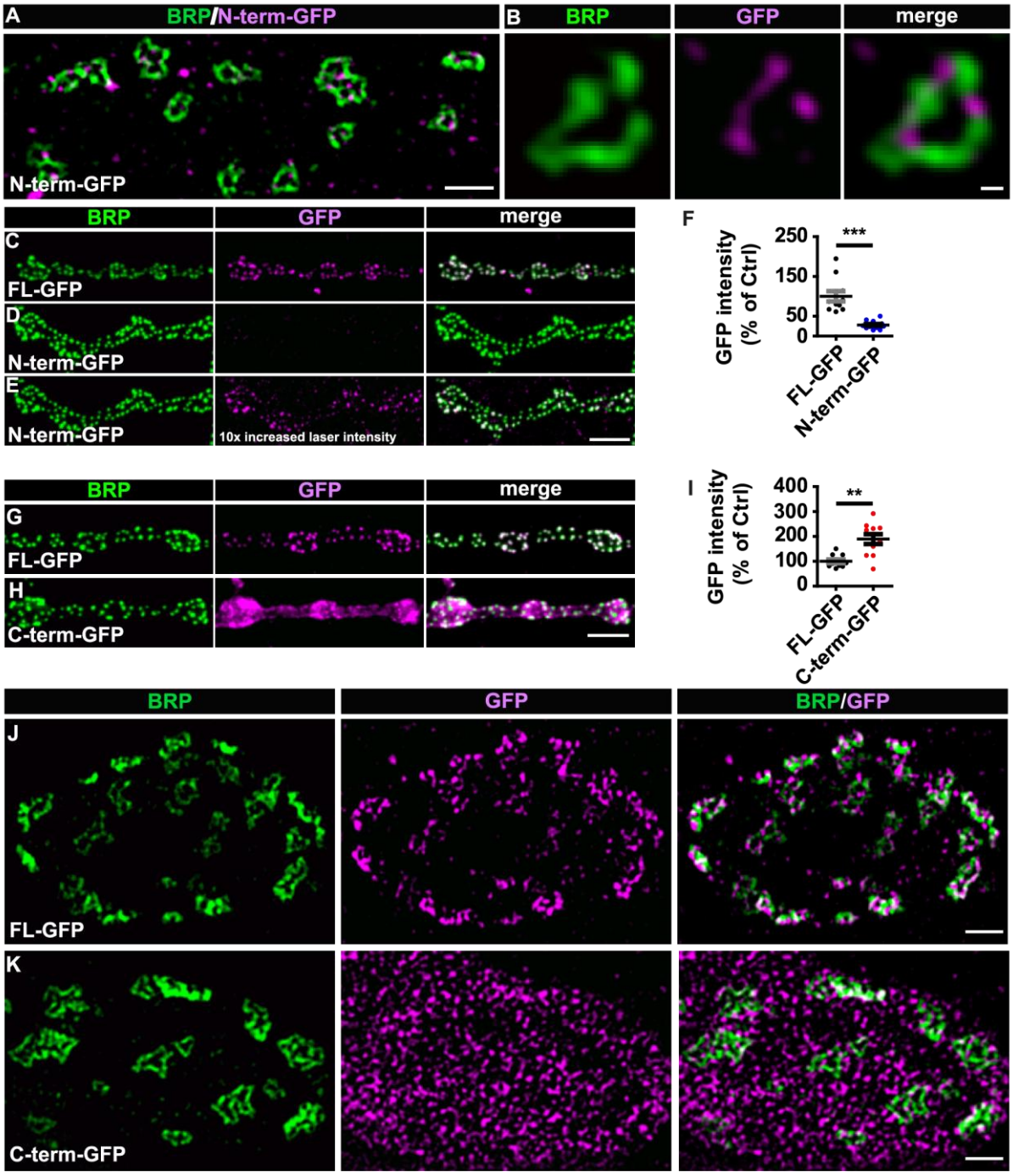

Figure S3: the N-term-GFP fragment but not the C-term-GFP fragment localized specifically to AZs

(A,B) Two-color STED image of synaptic bouton (A) and single AZs (B) from 3rd instar larvae pan-neuronally overexpressing N-term-GFP stained with the indicated antibodies. **(C-E)** Muscle 4 NMJs of segment A2-4 from 3rd instar Wild-type larvae pan-neuronally overexpressing FL-GFP (C) or N-term-GFP (D,E) labelled with the indicated antibodies. In (E) the laser intensity exciting the GFP staining was increased 10x in comparison to FL-GFP. **(F)** Quantification of GFP intensity measured over the whole NMJ in both conditions. **(G,H)** Muscle 4 NMJs of segment A2-4 from 3rd instar *unc13*^{null} larvae pan-neuronally expressing FL-GFP (G) or C-term-GFP (H) labelled with the indicated antibodies. **(I)** Quantification of GFP intensity measured over the whole NMJ in

both conditions. **(J,K)** Two-color STED image of a synaptic bouton from 3rd instar *unc13*^{null} larvae pan-neuronally expressing FL-GFP (J) or C-term-GFP (K) stained with the indicated antibodies. Figure source data, number of experiments and P values are listed in **Supplementary Table 1**. Scale bar: (A,J,K) 500 nm; (B) 50 nm; (C-E; G,H) 5 µm. Statistics (F,I): Mann-Whitney U test. $^{**}P \leq 0.01$; $^{***}P \leq 0.001$; ns, not significant, $P > 0.05$. All panels show mean ± s.e.m..

Figure S4 – related to Figure 4

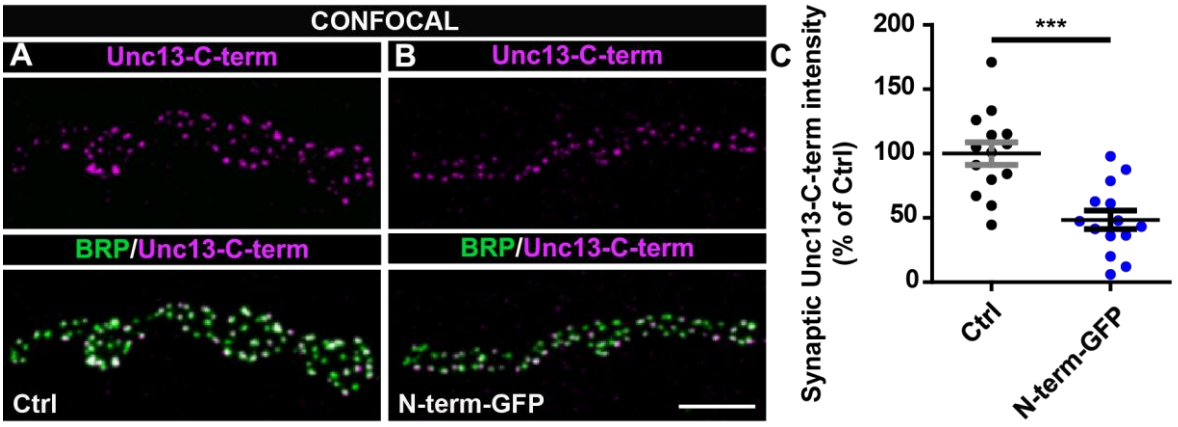

Figure S4: overexpression of N-term-GFP displaces endogenous Unc13 from the AZ

(A,B) Muscle 4 NMJs of segment A2-4 from 3rd instar larvae of Ctrl (A) and pan-neuronally overexpressing N-term-GFP (B) labelled with the indicated antibodies. **(C)** Quantification of synaptic Unc13-C-term intensity for Ctrl and pan-neuronally overexpressed N-term-GFP. Figure source data, number of experiments and P values are listed in **Supplementary Table 1**. Scale bar: 5 µm. Statistics: Mann-Whitney U-test. ***$P \leq 0.001$. Panel shows mean ± s.e.m.

Figure S5 – related to Figure 5

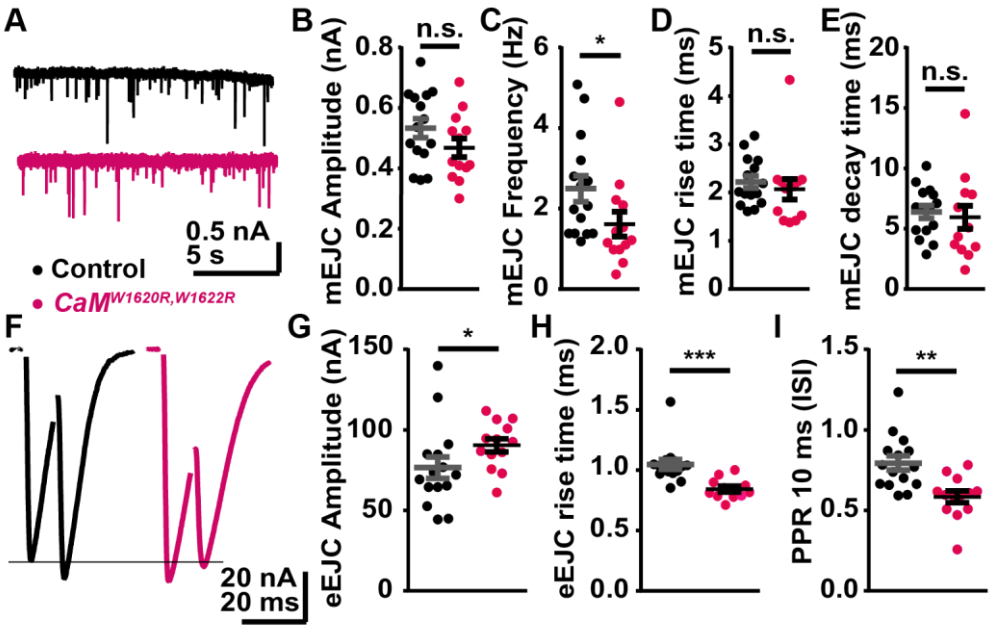

Figure S5: influence of CaM-binding site mutation in Unc13A on synaptic transmission

(A) Representative mEJC traces for Control (black) and *CaM*^{W1620R,W1622R} (magenta) cells. **(B-E)** mEJC amplitudes (B), frequencies (C), rise times (10% to 90%; (D)), and decays (E) in Control and *CaM*^{W1620R,W1622R}. **(F)** Representative eEJC traces for Control and *CaM*^{W1620R,W1622R} cells. **(G-I)** Quantification of eEJC amplitudes (G), rise times (10% to 90%; H)), and paired pulse ratios with 10 ms ISI (I) in Control and *CaM*^{W1620R,W1622R} cells. Figure source data, number of experiments and P values are listed in **Supplementary Table 1**. Statistics: Mann-Whitney U test. *P ≤ 0.05; **P ≤ 0.01; ***P ≤ 0.001; ns, not significant, P > 0.05. All panels show mean ± s.e.m.

Figure S6 – related to Figure 5

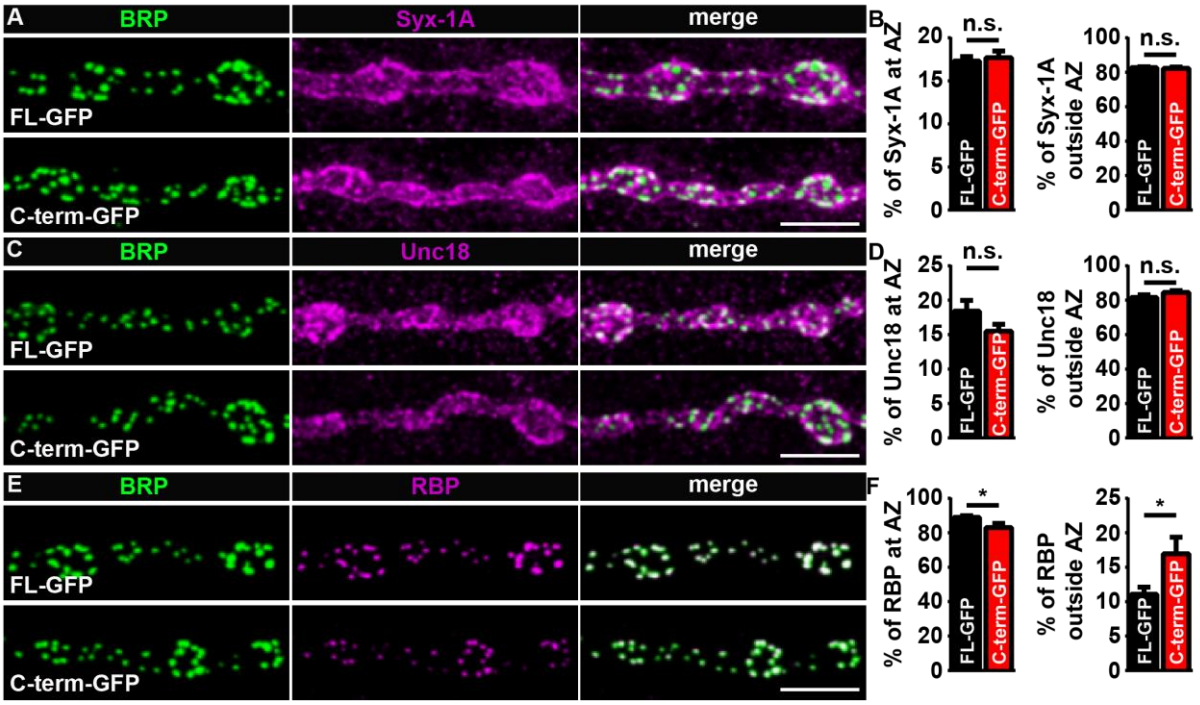

Figure S6: C-term-GFP redistributed RBP from the AZ

(A,C,E) Muscle 4 NMJs of segment A2-4 from 3rd instar *unc13*^{null} larvae pan-neuronally expressing FL-GFP or C-term-GFP labelled with the indicated antibodies. **(B,D,F)** Quantification of percentage of Syx-1A (B), Unc18 (D) and RBP (F) in- and outside of the AZ. Figure source data, number of experiments and P values are listed in **Supplementary Table 1**. Scale bar: 5 µm. Statistics: Mann-Whitney U-test. *$P \leq 0.05$; ns, not significant, $P > 0.05$. Panel shows mean ± s.e.m.

Figure S7 – related to Figure 6

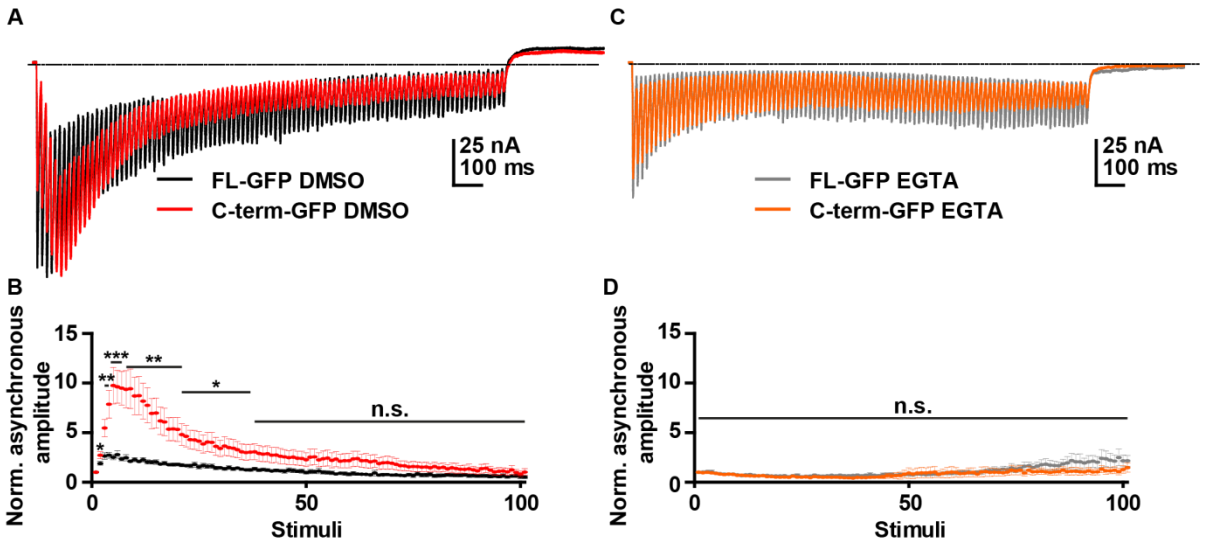

Figure S7: synaptic transmission upon rescue with C-term-GFP has augmented asynchronous release which is abolished by EGTA treatment

(A) Average eEJC traces of *unc13*^{null} larvae expressing FL-GFP (control, black) or C-term-GFP (red) in the absence of EGTA in response to 60 Hz trains (extended view of traces in Figure 6A, here showing all responses). **(B)** Normalized asynchronous amplitude plotted against stimulus number without EGTA in both genotypes. **(C)** Average eEJC traces for FL-GFP (control, grey) and C-term-GFP (orange) expressing *unc13*^{null} larvae in the presence of EGTA in response to 60 Hz trains (extended view of traces in Figure 6G, here showing all responses). **(D)** Normalized asynchronous amplitude plotted against stimulus number for FL-GFP and C-term-GFP in the presence of EGTA. Figure source data, number of experiments and P values are listed in **Supplementary Table 1**. Statistics: t test. *$P \leq 0.05$; **$P \leq 0.01$; ***$P \leq 0.001$; ns, not significant, $P > 0.05$. All panels show mean ± s.e.m. The extracellular solution contained 2.5 mM Ca^{2+}.

Figure S8 – related to Figure 6

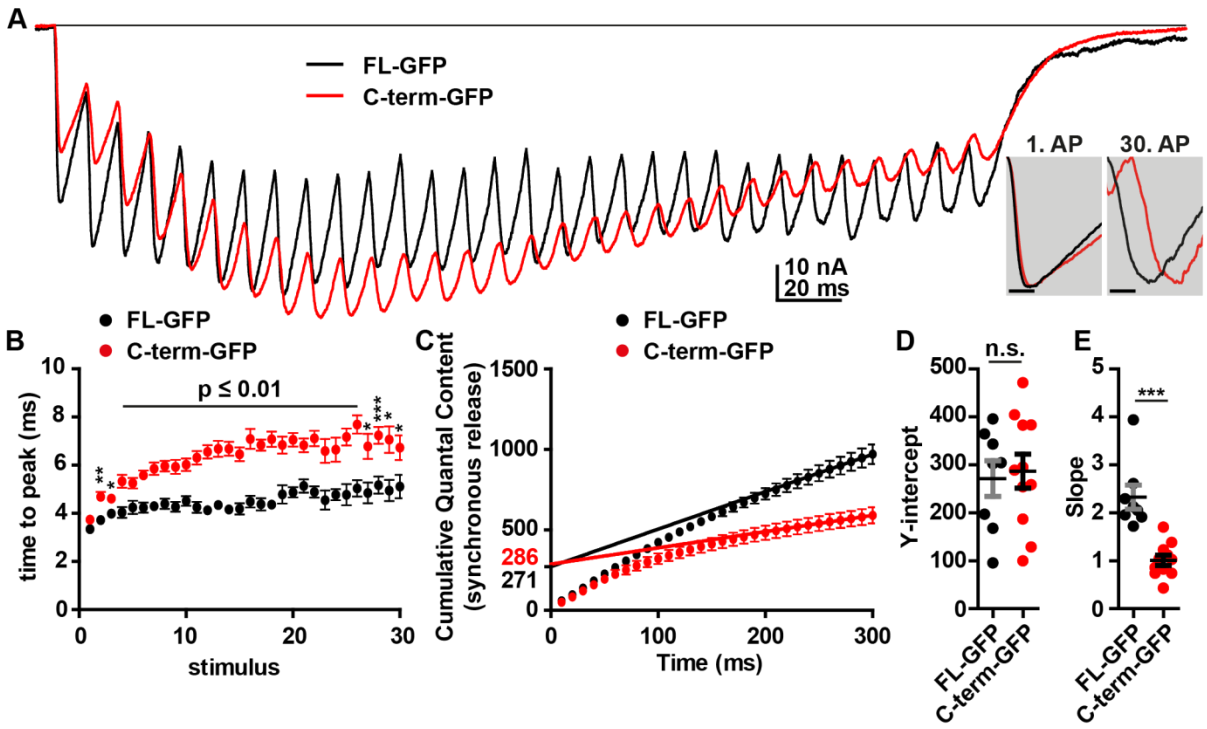

Figure S8: asynchronous and delayed release and slower forward priming in *unc13*^{null} larvae expressing the C-term-GFP fragment

(A) Average eEJC traces of *unc13*^{null} larvae expressing FL-GFP (control, black) or C-term-GFP (red) in response to 100 Hz trains, 30 APs. Inlets show average, normalized eEJC amplitudes to the first stimulus and to the 30th stimulus of FL-GFP (black) and C-term-GFP (red) expressing cells to illustrate effects on the time course of release. **(B)** Time-to-peak (ms) for FL-GFP (control, black) and C-term-GFP (red) conditions plotted against stimuli number. **(C)** Cumulative quantal content (synchronous release divided by mean mEJC amplitudes in each genotype) plotted against time (ms) in both genotypes. Lines represent the best fit to all data in each genotype, fits restricted to 260-300 ms. **(D)** Cell-wise quantification of y-intercepts from linear fits from individual cells of either genotype. **(E)** Cell-wise quantification slopes of linear fits in individual cells of either genotype. The slope was significantly larger in FL-GFP compared to C-term-GFP. Figure source data, number of experiments and P values are listed in **Supplementary Table 1**. Statistics: t test. *$P \leq 0.05$; **$P \leq 0.01$; ***$P \leq 0.001$; ns, not significant, $P > 0.05$. All panels show mean ± s.e.m.. The extracellular solution contained 1.5 mM Ca^{2+}.